http://dx.doi.org/10.5012/bkcs.2013.34.9.2731

Tetrameric Self-Assembly of a Cu(II) Complex Containing Schiff-Base Ligand and Its Unusually High Catecholase-like Activity

Shuranjan Sarkar, Woo Ram Lee,† Chang Seop Hong,† and Hong-In Lee*

Department of Chemistry and Green-Nano Materials Research Center, Kyungpook National Univeristy, Daegu 702-701, Korea
**E-mail: leehi@knu.ac.kr*
†Department of Chemistry, Research Institute for Natural Sciences, Korea University, Seoul 136-713, Korea
Received May 31, 2013, Accepted June 24, 2013

We report a new tetrameric supramolecular Cu(II) complex (Cu_4L_4 = tetrakis(*N,N′*-bis(salicylidene)-2,2'-ethylenedianiline)Copper(II)) with a Schiff-base ligand (H_2L = *N,N′*-bis (salicylaldimine)-1,2-ethylenediamine) containing two N,O-bidentate chelate groups. Though the copper sites of Cu_4L_4 are non-coupled, the complex exhibits a unsually high catecholase-like activity (k_{cat} = 935 h^{-1}) when the Cu_4L_4 solution is treated with 3,5-di-*tert*-butylcatechol (3,5-DTBC) at basic condition in the presence of air. Combined information obtained from UV-VIS and EPR measurements could lead the suggestion of the reaction pathway in which the substrate may bind to Cu(II) ions by *anti-anti* didentate bridging mode.

Key Words : Cu(II) complex, N,O-ligand, Self-assembly, Cu(II) EPR, Catecholase

Introduction

Multicopper enzymes containing more than one copper ion in their active sites are widely utilized in nature for transporting copper ions, transferring electrons, activating dioxygen molecules, and catalyzing many reactions.[1-3] Catechol oxidase, one of the multicopper enzymes, is a type-3 copper protein which catalyzes the oxidation of catechols to the corresponding *o*-quinones.[4] The active site of the enzyme contains a dinuclear copper center. Each copper ion is coordinated by three histidine nitrogen atoms, joined by a hydroxy bridge with Cu(II)-Cu(II) distance of 2.9 Å in the oxidized (*met*) form. But in the reduced (*deoxy*) form, the Cu(I)-Cu(I) separation increases to 4.4 Å and a water molecule coordinates to one of the copper ions.[4-7] Numerous model compounds for this enzyme have been reported.[4,8-13] All over these works, the effect of various structural factors on the catecholase activity has been analyzed, but up to now there are no concluding results that could recognize the structural features that enhance catalytic activity. One of the ways to understand the nature of the multicopper enzymes is the construction and characterization of model compounds. Recent development of metal-assisted self-assembly has made enormous success in mimicking the multicopper enzymes.[14,15] We have synthesized a new Schiff-base ligand (H_2L = *N,N′*-bis(salicylaldimine)-1,2-ethylenediamine) containing two N,O-bidentate chelate groups linked by a spacer. By controlling the length and rigidity of the spacer, we could successfully build a tetrameric supramolecular Cu(II) complex (Cu_4L_4 = tetrakis(*N,N′*-bis(salicylidene)-2,2'-ethylenedianiline)Copper(II)). Single crystal X-ray crystallography of Cu_4L_4 revealed that the copper sites were non-coupled, however, the complexes showed unexpectedly-high catecholase-like activity when Cu_4L_4 was treated with 3,5-di-*tert*-butylcatechol (3,5-DTBC) in the presence of air at basic condition. In this paper, we report the structure and catecholase-like activity of the complex investigated by UV/VIS and electron paramagnetic resonance (EPR) spectroscopies.

Experimental

Synthesis of *N,N′*-Bis(salicylidene)-2,2'-ethylenedianiline (H_2L). The ligand, H_2L, was prepared by slight modification of the literature method.[16] A solution of salicylaldehyde (0.75 g, 6.0 mmol) dissolved in 5 mL of dry toluene was added to a magnetically-stirred solution of 2,2'-ethylenedianiline (0.66 g, 3.0 mmol) dissolved in 20 mL of dry toluene. The mixture solution was refluxed for 2 h. Yellow solid products were washed several times with methanol and dried under a vacuum at ambient temperature. Yield: 90% (1.3 g), mp > 200 °C. The H_2L ligand was identified by FT-IR recorded from a KBr pellet and ^1H and ^{13}C NMR recorded in $CDCl_3$ at 25 °C showing identical features to the previously reported data.[16] ^1H NMR (400 MHz, $CDCl_3$, 298 K) δ 13.22 (s, 2H, O*H*), 8.07 (s, 2H, NC*H*), 7.40-6.81 (m, 6H, Ar*H*), 3.04 (s, 4H, N(PhCH_2CH_2Ph)N). ^{13}C NMR (400 MHz, $CDCl_3$, 298 K) δ 162.92 (N*C*H), 161.41 (Ar*C*), 148.04 (Ar*C*), 135.50 (Ar*C*), 133.37 (Ar*C*), 132.73 (Ar*C*), 130.81 (Ar*C*), 127.64 (Ar*C*), 127.22 (ArC), 119.76 (Ar*C*), 119.35 (Ar*C*), 118.30 (Ar*C*H), 117.65 (Ar*C*), 33.50 (N(Ph*C*H_2*C*H_2Ph)N). NMR (400 MHz) spectra were recorded on a Bruker Advance Digital 400-NMR spectrometer and chemical shifts were recorded in *ppm* units.

Synthesis of Tetrakis((*N,N′*-bis(salicylidene)-2,2'-ethylenedianiline)Copper(II)·4(CH_3OH) (Cu_4L_4·4(CH_3OH)). A solution of $Cu(ClO_4)_2·6H_2O$ (0.76 g, 2.0 mmol) dissolved in 10 mL of dry methanol was added dropwise to a methanolic solution of H_2L (0.84 g 2.0 mmol) and sodium hydroxide (0.16 g 4.0 mmol). The mixture solution was refluxed half an hour. After stirring over night at ambient

temperature, gold matte crystalline powder was collected by filtration. Yield: 80% (0.8 g), mp > 200 °C. The powder was again dissolved in acetonitrile to be taken 5×10^{-4} M 5 mL in a vial. Suitable crystals for an X-ray analysis were obtained from the solution after one week. Elemental analysis calculated for $C_{116}H_{104}Cu_4N_8O_{12}$ (mol. wt. = 2056.23): C, 67.76%; H, 5.10%; N, 5.45%. Found: C, 68.42%; H, 4.53%; N 5.73%. Positive ion FAB MS analysis (*m/z*, ion, base): 483.10, $\{[CuL+H]^+\}$, 15%, 965.3, $\{[Cu_2L_2+H]^+\}$, 100%, 1928.13 $\{[Cu_4L_4+H]^+\}$, 0.5%. The elemental analysis was done using a Perkin-Elmer 2400 CHN analyzer.

X-Ray Crystallography. X-ray data for $Cu_4L_4{\cdot}4CH_3OH$ was collected on a Bruker SMART APEXII diffractometer equipped with graphite monochromated MoK_α radiation (λ = 0.71073 Å). Preliminary orientation matrix and cell parameters were determined from three sets of ω scans at different starting angles. Data frames were obtained at scan intervals of 0.5° with an exposure time of 10 s per frame. The reflection data were corrected for Lorentz and polarization factors. Absorption corrections were carried out using SADABS.[17] The structures of $Cu_4L_4{\cdot}4CH_3OH$ was solved by direct methods and refined by full-matrix least-squares analysis using anisotropic thermal parameters for non-hydrogen atoms with the SHELXTL program.[18] All hydrogen atoms were calculated at idealized positions and refined with the riding models. A summary of the crystal and some crystallographic data for $Cu_4L_4{\cdot}4CH_3OH$ are listed in Table 1. Crystallographic data for the structures reported here have been deposited with CCDC (Deposition No. CCDC-891321). These data can be obtained free of charge from The Cambridge Crystallographic Data Centre *via* www.ccdc.cam.ac.uk/data_request/cif.

EPR Experiment. X-band (9 GHz) electron paramagnetic resonance (EPR) spectra were collected on a Jeol JES-TE300 ESR spectrometer using a 100 kHz field modulation. Low temperature spectra were obtained using a Jeol ES-DVT3 variable temperature controller. The spectral simulations were performed using the program *EasySpin*.[19]

Results and Discussion

The ligand, H_2L, used for synthesizing Cu_4L_4 was prepared by slight modification of the literature method.[16] A gold matte powder of $Cu_4L_4{\cdot}4(CH_3OH)$ was obtained by adding a methanolic solution of $Cu(ClO_4)_2{\cdot}6H_2O$ into a methanolic solution of H_2L (Scheme 1).

Figure 1 shows the Cu_4L_4 structure in the crystal of $Cu_4L_4{\cdot}4(CH_3OH)$. Overall architecture is constructed by cyclization of four CuL units (Scheme 1). Each L^{2-} ligand bridges two Cu(II) ions *via* two outward salicylaldimine groups. Each Cu(II) ion is tetradentately coordinated by two sets of N and O atoms, originating from two different L^{2-} ligands. The Cu-N bond lengths are in the range of 1.979(4)-1.995(7) Å and the Cu-O bond lengths are in the range of 1.864(3)-1.896(3) Å. The bond angles of O-Cu-O, N-Cu-N, and N-Cu-O lie between 152.1(2)°-165.7(2)°, 154.3(2)°-162.4(2)°, and 89.0(2)°-94.5(2)°, respectively, showing that the coordination geometries are distorted square planar. The selected bond length and angles for this complex are listed in

Table 1. Crystal data and structure refinement for $[Cu_4L_4]{\cdot}4CH_3OH$

Empirical formula	$C_{116}H_{104}Cu_4N_8O_{12}$
Formula weight	2056.23
Temperature, K	100
Wavelength, Å	0.71073
Crystal system	Monoclinic
Space group	*P*21/n
a, Å	15.014(2)
b, Å	23.942(2)
c, Å	28.591(2)
β, °	104.426(2)
Volume, Å^3	9953 (1)
Z	4
Independent Reflections	24480 (R_{int} = 0.1466)
Goodness-of-fit on F^2	1.021
Final *R* indices $[I > 2\sigma(I)]^{a,b}$	R_1 = 0.0672, wR_2 = 0.1478
R indices (all data)	R_1 = 0.1633, wR_2 = 0.1884
Largest diff. peak and hole, e·Å^{-3}	1.321 and –0.920

$^aR_1 = \Sigma||F_0|-|F_c||/\Sigma|F_0|$. $^bwR_2 = [\Sigma w(F_0^2-F_c^2)^2/\Sigma wF_0^4]^{1/2}$

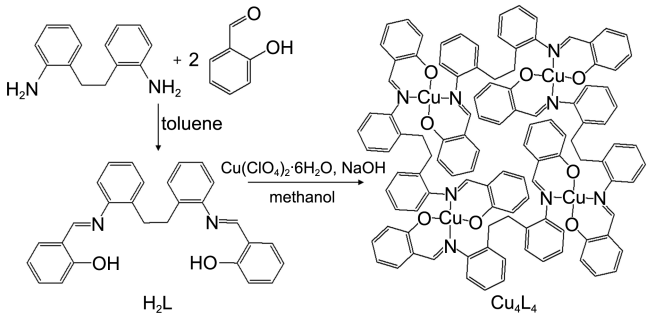

Scheme 1

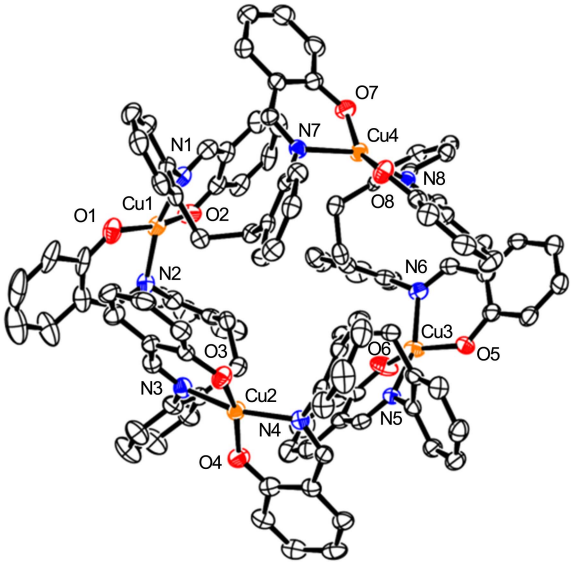

Figure 1. ORTEP diagram of Cu_4L_4 with 33% probability ellipsoids and atom numbering scheme. Hydrogen atoms have been omitted for clarity.

Table 2. Selected bond lengths and angles for $Cu_4L_4 \cdot 4(CH_3OH)$

	Bond lengths (Å)		
Cu1-O1	1.879(3)	Cu1-N1	1.995(4)
Cu1-O2	1.892(3)	Cu1-N2	1.988(4)
Cu2-O3	1.896(3)	Cu2-N3	1.994(4)
Cu2-O4	1.879(3)	Cu2-N4	1.989(4)
Cu3-O5	1.864(3)	Cu3-N5	1.985(4)
Cu3-O6	1.882(4)	Cu3-N6	1.966(4)
Cu4-O7	1.894(3)	Cu4-N7	1.979(4)
Cu4-O8	1.874(3)	Cu4-N8	1.990(4)
	Bond angles (°)		
O1-Cu1-O2	165.7(2)	N1-Cu1-N2	162.4(2)
O1-Cu1-N1	89.0 (2)	O1-Cu1-N2	92.2(2)
O2-Cu1-N1	93.1(2)	O2-Cu1-N2	90.1(2)
O3-Cu2-O4	159.5(2)	N3-Cu2-N4	162.2(2)
O3-Cu2-N3	92.5(2)	O3-Cu2-N4	91.6(2)
O4-Cu2-N3	89.5(2)	O4-Cu2-N4	92.8(2)
O5-Cu3-O6	152.1(2)	N5-Cu3-N6	155.0(2)
O5-Cu3-N5	91.0(2)	O5-Cu3-N6	93.0(2)
O6-Cu3-N5	93.4(2)	O6-Cu3-N6	92.2(2)
O7-Cu4-O8	153.7(2)	N7-Cu4-N8	154.3(2)
O7-Cu4-N7	93.3(2)	O7-Cu4-N8	94.5(2)
O8-Cu4-N7	90.1(2)	O8-Cu4-N8	93.7(2)

Table 2.

Four Cu(II) ions are arranged to form a distorted tetrahedron as depicted in Figure 2. The distances between the copper ions bridged by one L^{2-} ligand (Cu1···Cu2, Cu2···Cu3, Cu3···Cu4, Cu4···Cu1) are 7.073-7.319 Å. The distances between the non-bridged copper ions (Cu1···Cu3, Cu2···Cu4) are a little longer with 8.595-8.957 Å. Cu···Cu···Cu angles within the supramolecular cycle (Cu1···Cu2···Cu3, Cu2···Cu3Cu4, Cu3···Cu4···Cu1, Cu4···Cu1···Cu2) are in the range of 72.5°-77.6° and all the other Cu···Cu···Cu angles lie within 50.5°-54.3°. Similar tetrameric assemblies constructed from Cu(II) ions and bis(N,O-bidenate) Schiff-base ligands have been reported.[15,20,21] The structures of the tetrameric copper complexes depended on the spacer groups, which connect two N,O-bidenate ligands, of the bis(N,O-bidenate) Schiff-base ligands. When the complexes with rigid spacers were stabilized by weak aromatic π-π and CH-π, the metal ions were almost coplanar in rhombic arrangements,[15,20] whereas in the complex with a flexible spacer group the metal ions were arranged in a tetrahedral arrangement.[21] Cu_4L_4, where two N,O-bidentate ligands are linked by a flexible phenyliminomethylphenoxy group, forms a similar shape to the latter.

For investigating the catecholase-like activity of Cu_4L_4, Cu_4L_4 solution in acetonitrile was treated with 3,5-di-*tert*-butylcatechol (3,5-DTBC) in the presence of air at pH 8. The product, 3,5-di-*tert*-butyl-*o*-quinone (3,5-DTBQ), is considerably stable and has a strong absorption at $\lambda_{max} = 400$ nm ($\varepsilon = 1{,}900\ M^{-1}cm^{-1}$),[14] so that the activity and reaction rate, respectively, could be determined using UV-VIS spectroscopy. Figure 3 shows the change of UV-VIS spectra at room temperature upon adding 4.5×10^{-4} M (1.35×10^{-6} mol) 3,5-DTBC into the 2.5×10^{-5} M (7.5×10^{-8} mol) Cu_4L_4. As observed in the figure, the quinone band at 400 nm increases over time. The amount of 3,5-DTBQ generated by the reaction was 1.2×10^{-6} mol which is much more than the amount of Cu_4L_4, indicating the catalytic activity of Cu_4L_4.

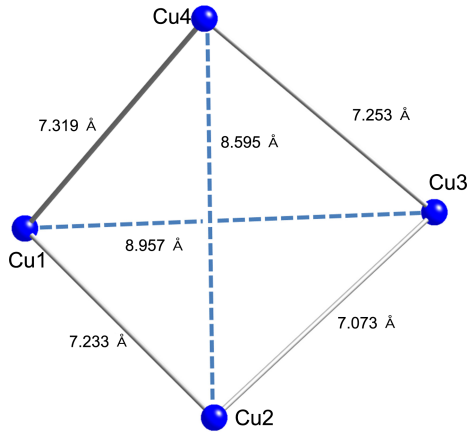

Figure 2. Arrangement of four Cu(II) sites in Cu_4L_4.

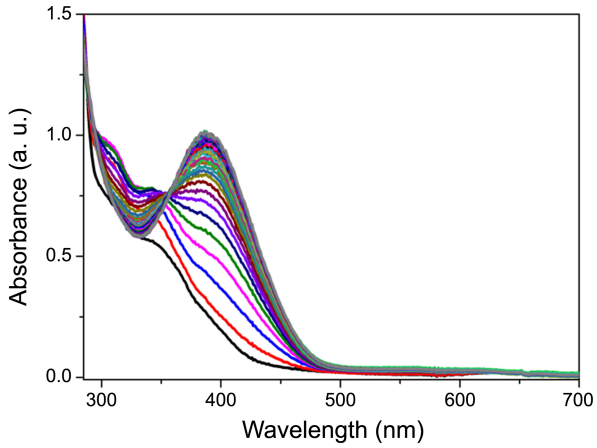

Figure 3. Change of UV-VIS absorption spectra of Cu_4L_4 + 3.5-DTBC. The reaction was initiated by adding 6.25×10^{-4} M (1.88×10^{-6} mol) 3,5-DTBC into 6.25×10^{-6} M (1.88×10^{-8} mol) Cu_4L_4. Each spectrum was obtained every 20 second up to 800 seconds after mixing.

The kinetic study of the oxidation of 3,5-DTBC by Cu_4L_4 was carried out using the initial rate method (Figure 4). Figure 4(c) is the corresponding Lineweaver-Burk plot obtained from the initial rates when 2.5×10^{-5} M Cu_4L_4 solution was mixed with 0.5-24 equivalents of 3,5-DTBC. Kinetic parameters of $V_{max} = 6.5 \times 10^{-6}\ Ms^{-1}$, $K_M = 2.05 \times 10^{-4}$ M, $k_{cat} = 0.26\ s^{-1}$, and $k_{cat}/K_M = 1268\ s^{-1}M^{-1}$ were calculated based on Michaelis-Menten model. Previous studies on catecholase activities of copper model complexes have showed wide range of k_{cat} values from less than 1 h^{-1} to 9471 h^{-1}.[22] k_{cat} value of 935 h^{-1} (= 0.26 s^{-1}) observed from Cu_4L_4 is comparable to those with moderate to high catecholase activities.[8-13,23-41] It is noticeable that the four copper ions are non-coupled in Cu_4L_4 whereas most model complexes with high catecholase activities are di- or tri-nuclear copper

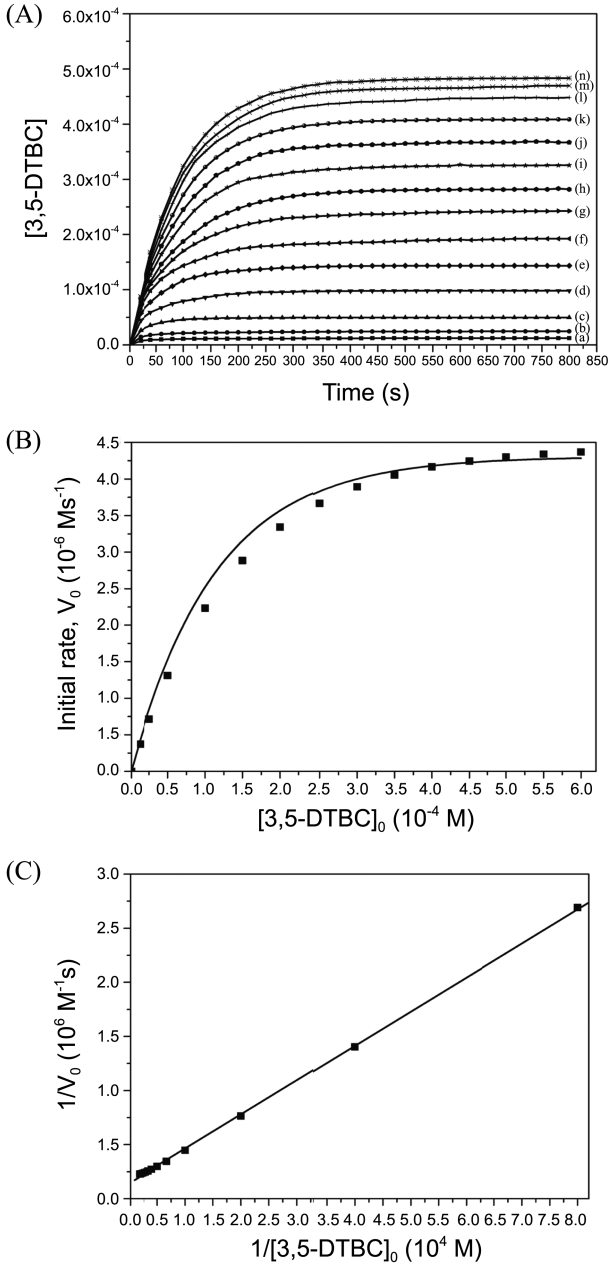

Figure 4. Kinetic study of oxidation of 3,5-DTBC by Cu_4L_4. $[Cu_4L_4]_0 = 2.5 \times 10^{-5}$ M (A) [3,5-DTBQ] *vs.* time. Concentrations of 3,5-DTBQ were calculated from the absorbance at λ_{max} = 400 nm (ε = 1,900 $M^{-1}cm^{-1}$). $[3,5\text{-DTBC}]_0$ = (a) 1.25×10^{-5} M, (b) 2.50×10^{-5} M, (c) 5.0×10^{-5} M, (d) 1.0×10^{-4} M, (e) 1.5×10^{-4} M, (f) 2.0×10^{-4} M, (g) 2.5×10^{-4} M, (h) 3.0×10^{-4} M, (i) 3.5×10^{-4} M, (j) 4.0×10^{-4} M, (k) 4.5×10^{-4} M, (l) 5.0×10^{-4} M, (m) 5.5×10^{-4} M and (i) 6.0×10^{-4} M. (B) Initial reaction rates of oxidation of 3,5-DTBC *vs.* $[3,5\text{-DTBC}]_0$. (C) Corresponding Lineweaver-Burk plot.

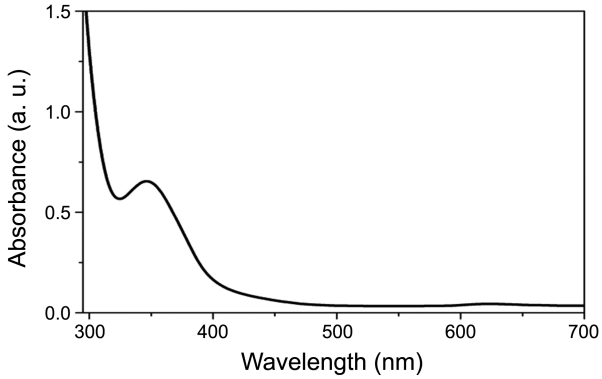

Figure 5. Detection of H_2O_2 through iodometric method.

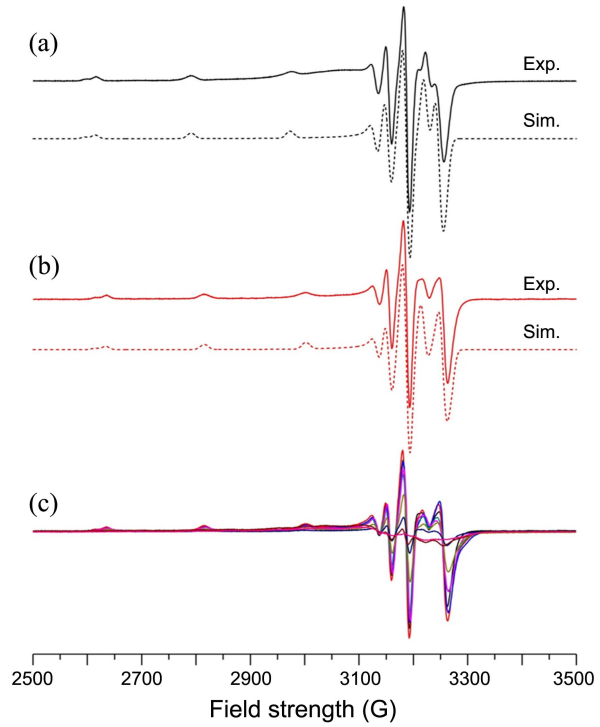

Figure 6. (a) EPR spectrum of Cu_4L_4 solution containing aqueous sodium hydroxide in CH_3CN and corresponding numerical simulation. (b) EPR spectrum obtained from the reaction mixture at 25 sec after adding 3,5-DTBC into the Cu_4L_4 solution and corresponding numerical simulation. (c) Overlay of the EPR spectra obtained from the reaction mixture at 25 sec, 1 min, 5 min, 10 min, 15 min, 20 min, 30 min, and 50 min, 120 min after the initial reaction. $[Cu_4L_4]_0 = 3.4 \times 10^{-4}$ M, $[3,5\text{-DTBC}]_0 = 6.8 \times 10^{-3}$ M. EPR experimental conditions: microwave frequency, 9.13 GHz; microwave power, 1 mW; modulation amplitude, 2.5 G; time constant, 0.3 sec; scan speed, 500 G/min; temperature, 110 K. Simulation parameters: (a) g = [2.050 2.050 2.263]; A^{Cu} = [83 83 565] MHz; Gaussian linewidth (HWHF) = 15 G and (b) g = [2.050 2.050 2.242]; A^{Cu} = [75 75 575] MHz.

complexes.

During the catalytic oxidation of 3,5-DTBC in some model complexes, H_2O_2 have been often detected, which gave insight into the reaction pathway.[4,42,43] For further understanding of oxidation pathway of 3,5-DTBC by Cu_4L_4, we have tested the formation of H_2O_2 using iodometric method.[8,9,24] The reaction was initiated by adding 3,5-DTBC into a basic CH_3CN solution of Cu_4L_4. The resulting concentrations of 3,5-DTBC and Cu_4L_4 were 1.0×10^{-3} M (1.0×10^{-5} mol) and 1.0×10^{-4} M (1.0×10^{-6} mol), respectively, and total volume of the solution was 10 mL. After 40 min of reaction, an equal volume of water was added, and 3,5-DTBQ formed during the reaction and residual 3,5-DTBC were extracted three times with dichloromethane. The

aqueous layer was acidified with H_2SO_4 to pH = 2 to stop further reaction. 1 mL of a 10% solution of KI and three drops of 3% solution of ammonium molybdate were added into the aqueous layer. Presence of H_2O_2 could be monitored spectrophotometrically by the development of the characteristic I_3^- band at λ_{max} = 353 nm (=26,000 M^{-1} cm^{-1}) by the reaction, $H_2O_2 + 2I^- + 2H^+ \rightarrow 2H_2O + I_2$, and $I_2 + I^- \rightarrow I_3^-$. For UV-VIS experiment, 0.1 mL of the aqueous mixture was taken into 3 mL H_2O in the UV cell. Calculated $[I_3^-] = 2.5 \times 10^{-5}$ M = $[H_2O_2]$, implying that 8.3×10^{-6} mol of H_2O_2 was generated from the original Cu_4L_4 + 3,5-DTBC reaction, implying about 0.8 mol of H_2O_2 was generated per one mol of 3,5-DTBC consumed during the reaction as depicted in Figure 5.

For further investigation of the reaction pathway, ERP measurements were also performed during the course of the oxidation of 3,5-DTBC by Cu_4L_4. Figure 6 shows the spectra obtained from 3×10^{-4} M Cu_4L_4 solution containing sodium hydroxide (Figure 6(a)) and the reaction mixture trapped at 25 sec after adding 3,5-DTBC into the Cu_4L_4 solution (Figure 6(b)). EPR of Cu_4L_4 solution in basic condition could be well simulated with g = [2.050 2.050 2.263] and $\boldsymbol{A}^{Cu}$ = [83 83 565] MHz. The spectrum is highly axial and has g-values of $g_{\parallel} > g_{\perp} > 2$, indicating the Cu coordination is a tetragonal, square planar or square pyramidal geometry. Upon addition of 3,5-DTBC into the solution, EPR feature is slightly changing to show a new signal with g = [2.050 2.050 2.242] and $\boldsymbol{A}^{Cu}$ = [75 75 575] MHz. This EPR signal was gradually decreasing over time, as shown in Figure 6(c).

Cumulative information obtained from the UV-VIS and EPR measurements could lead the suggestion of the reaction pathway of the catecholase-like activity as depicted in Figure 7. The catecholase-like activity of the complex was not observed without increasing pH of the reaction mixture by adding aqueous sodium hydroxide. Upon addition of aqueous sodium hydroxide into the solution of Cu_4L_4, EPR spectrum was changed from its original spectrum to Figure 6(a), implying the Cu(II) coordination environments were modified by hydroxide ion, which activated the complex for the catalytic action (Cu_4L_4-OH). When 3,5-DTBC was added, EPR spectrum was slightly changed while most of its EPR features remained the same (Figure 6(b)). Considering *ca*. 7 Å of the distances between two nearby Cu(II) ions, it is a good fit for 3,5-$DTBC^{2-}$ bridging two Cu(II) ions *via anti-anti* didentate binding mode (Cu_4L_4-DTBC). Next, the substrate is oxidized to 3,5-DTBQ and the complex is reduced (*red*-Cu_4L_4). After the catalyst goes through a peroxo-bound form (Cu_4L_4-O_2^{2-}), the substrate kicks out hydrogen peroxide to form Cu_4L_4-DTBC. More detailed mechanistic studies using high resolution ESI-MS are underway.

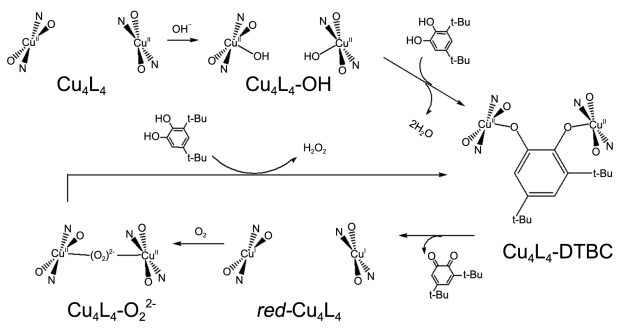

Figure 7. Suggested reaction pathway of the catecholase-like activity of Cu_4L_4.

Conclusion

In summary, we have designed a Schiff-base ligand, H_2L, containing two N,O-bidentate chelate groups linked by a spacer to build a tetrameric supramolecular Cu(II) complex, Cu_4L_4. Single crystal X-ray crystallography of Cu_4L_4 revealed that the copper sites were non-coupled and arranged to form a distorted tetrahedron. The complex exhibited a catecholase-like activity when the Cu_4L_4 solution in acetonitrile was treated with 3,5-di-*tert*-butylcatechol (3,5-DTBC) at basic condition in the presence of air. Kinetic investigation found an unusually high catecholase-like activity of the complex though the copper sites are uncoupled. Combined information obtained from UV-VIS and EPR measurements could lead the suggestion of the reaction pathway in which the substrate may bind to Cu(II) ions by *anti-anti* didentate bridging mode. More detailed mechanistic studies using ESI-MS are underway.

Acknowledgments. This research was supported by Basic Science Research Program through the National Research Foundation of Korea (NRF) funded by the Ministry of Education, Science and Technology (2010-0024929) and Kyungpook National University Research Fund, 2012.

References

1. Solomon, E. I.; Chen, P.; Metz, M.; Lee, S.-K.; Palmer, A. E. *Angew. Chem. Int. Ed.* **2001**, *40*, 4570.
2. Solomon, E. I.; Sundaram, U. M.; Machonkin, T. E. *Chem. Rev.* **1996**, *96*, 2563.
3. Solomon, E. I.; Augustine, A. J.; Yoon, J. *Dalton Trans.* **2008**, 3921.
4. Koval, I. A.; Gamez, P.; Belle, C.; Selmeczi, K.; Reedijk, J. *Chem. Soc. Rev.* **2006**, *35*, 814.
5. Eicken, C.; Zippel, F.; Büldt-Karentzopoulos, K.; Krebs, B. *FEBS Lett*. **1998**, *436*, 293.
6. Rompel, A.; Fischer, H.; Büldt-Karentzopoulos, K.; Meiwes, D.; Zippel, F.; Nolting, H.-F.; Hermes, C.; Krebs, B.; Witzel, H. *J. Inorg. Biochem*. **1995**, *59*, 715.
7. Klabunde, T.; Eicken, C.; Sacchettini, J. C.; Krebs, B. *Nat. Struct. Biol*. **1998**, *5*, 1084.
8. Marion, R.; Zaarour, M.; Qachachi, N. A.; Saleh, N. M.; Justaud, F.; Floner, D.; Lavastre, O.; Geneste, F. *J. Inorg. Biochem*. **2011**, *105*, 1391.
9. Ackermann, J.; Buchler, S.; Meyer, F. *C. R. Chimie* **2007**, *10*, 421.
10. Belle, C.; Beguin, C.; Gautier-Luneau, I.; Hamman, S.; Philouze, C.; Pierre, J. L.; Thomas, F.; Torelli, S. *Inorg. Chem*. **2002**, *41*, 479.
11. Sreenivasulu, B.; Zhao, F.; Gao S.; Vittal, J. J. *Eur. J. Inorg. Chem*. **2006**, 2656.
12. Wang, X.; Ding, J.; Vittal, J. J. *Inorg. Chim. Acta* **2006**, *359*, 3481.
13. Panda, M. K.; Shaikh, M. M.; Butcher, R. J.; Ghosh, P. *Inorg. Chim. Acta* **2011**, *372*, 145.
14. Seneque, O.; Campion, M.; Douziech, B.; Giorgi, M.; Riviere, E.; Journaux, Y.; Mest, Y. L.; Reinaud, O. *Eur. J. Inorg. Chem.* **2002**,

2007.
15. Yoshida, N.; Oshio, H.; Ito, T. *J. Chem. Soc., Perkin Trans*. **2001**, *2*, 1674.
16. Hormnirun, P.; Marshall, E. L.; Gibson, V. C.; Pugh, R. I.; White, A. J. P. *Proc. Natl. Acad. Science* **2006**, *103*, 15343.
17. SADABS, *Area Detector Absorption Correction Program*, Bruker Analytical X-ray, Madison, WI, USA, 1997.
18. Sheldrick, G. M. *Acta Cryst.* **2008**, *A64*, 112.
19. Stoll, S.; Schweiger, A. *J. Magn. Reson.* **2006**, *178*, 42.
20. Yoshid, N.; Oshio, H.; Ito, T. *Chem. Commun*. **1998**, 63.
21. Halder, P.; Banerjee, P. R.; Zangrando, E.; Paine, T. K. *Eur. J. Inorg. Chem.* **2008**, 5659.
22. Wegner, R.; Gottschaldt, M.; Poppitz, W.; Jäger, E.-G.; Klemm, D. *J. Mol. Cat. A: Chem.* **2003**, *201*, 93.
23. Mijangos, E.; Reedijk, J.; Gasque, L. *Dalton Trans*. **2008**, 1857.
24. Neves, A.; Rossi, L. M.; Bortoluzzi, A. J.; Szpoganicz, B.; Wiezbicki, C.; Schwingel, E. *Inorg. Chem.* **2002**, *41*, 1788.
25. Peralta, R. A.; Neves, A.; Bortoluzzi, A. J.; Anjos, A. D.; Xavier, F. R.; Szpoganicz, B.; Terenzi, H.; Oliveira, M. C. B. de; Castellano, E.; Friedermann, G. R.; Mangrich, A. S.; Novak, M. A. *J. Inorg. Biochem*. **2006**, *100*, 992.
26. Gullotti, M.; Santagostini, L.; Pagliarin, R.; Granata, A.; Casella, L. *J. Mol. Cat. A Chem*. **2005**, *235*, 271.
27. Alves, W. A.; Almeida, S. A. de; Almeida, M. V. de; Paduan, A.; Becerra, C. C.; Ferreira, A. M. D. *J. Mol. Cat. A Chem*. **2003**, *198*, 63.
28. Oshi, N.; Nishida, Y.; Ida, K.; Kida, S. *Bull. Chem. Soc. Jpn*. **1980**, *53*, 2847.
29. Casellato, U.; Tamburini, S.; Vigato, P. A.; De Stefani, A.; Vidali, M.; Fenton, D. E. *Inorg. Chim. Acta* **1983**, *69*, 45.
30. Malachowski, M. R.; Davidson, M. G. *Inorg. Chim. Acta* **1989**, *162*, 199.
31. Kao, C.-H.; Wie, H.-H.; Liu, Y.-H.; Lee, G.-H.; Wang, Y.; Lee, C.-J. *J. Inorg. Biochem.* **2001**, *84*, 171.
32. Karlin, K. D.; Nasin, M. S.; Cohen, B. I.; Cruse, R. W.; Kaderli, S.; Zuberbuhler, A. D. *J. Am. Chem. Soc*. **1994**, *116*, 1324.
33. Karlin, K. D.; Wei, N.; Jung, B.; Kaderli, S.; Niklaus, P.; Zuberbuhler, A. D. *J. Am. Chem. Soc.* **1933**, *115*, 9506.
34. Battaini, G.; Monzani, E.; Casella, L.; Santagostini, L.; Pagliarin, R. *J. Biol. Inorg. Chem.* **2000**, *5*, 262.
35. Than, R.; Feldman, A. A.; Krebs, B. *Coord. Chem. Rev.* **1999**, *182*, 211.
36. Reim, J.; Krebs, B. *J. Chem. Soc., Dalton Trans*. **1997**, 3793.
37. Monzani, E.; Quinti, L.; Perotti, A.; Casella, L.; Gullotti, M.; Randaccio, L.; Geremia, S.; Nardin, G.; Faleschini, P.; Tabbi, G. *Inorg. Chem.* **1998**, *37*, 553.
38. Monzani, E.; Battaini, G.; Perotti, A.; Casella, L.; Gullotti, M.; Santagostini, L.; Nardin, G.; Randaccio, L.; Geremia, S.; Zanello, P.; Opromolla, G. *Inorg. Chem*. **1999**, *38*, 5359.
39. Wegner, R.; Gottschaldt, M.; Gorl, H.; Jager, E.-G.; Klemm, D. *Chem. Eur. J*. **2001**, *7*, 2143.
40. Mukherjee, J.; Mukherjee, R. *Inorg. Chim. Acta* **2002**, *337*, 429.
41. Neves, A.; Rossi, L. M.; Bortoluzzi, A. J.; Szpoganicz, B.; Wiezbicki, C.; Schwingel, E.; Haase, W.; Strovsky, S. *Inorg. Chem.* **2002**, *41*, 1788.
42. Chyn, J.-P.; Urbach, F. L. *Inorg. Chim. Acta* **1991**, *189*, 157.
43. Balla, J.; Kiss, T.; Jameson, R. F. *Inorg. Chem*. **1992**, *31*, 58.